

Efficient inhibition of cell proliferation and promotion of apoptosis requires continuous treatment with abemaciclib.

Authors: Torres-Guzmán Raquel¹, Ganado Maria Patricia¹, Mur Cecilia¹, Marugán Carlos¹, Baquero Carmen¹, Yang Yanzhu², Yi Zeng², Bian Huimin², Du Jian², de Dios Alfonso², Puig Oscar³, Lallena Maria Jose¹

Affiliations: ¹Discovery Chemistry Research & Technology, Eli Lilly and Company, Madrid, Spain; ²Eli Lilly and Company, Indianapolis, IN, USA; ³Eli Lilly and Company, New York, NY, USA

Abstract – 199/200 words

Abemaciclib is an oral, selective cyclin-dependent kinase 4 & 6 inhibitor (CDK4 & 6i), approved for hormone receptor-positive (HR+), human epidermal growth factor receptor 2-negative (HER2-) advanced breast cancer (ABC) as monotherapy for endocrine refractory disease, and with endocrine therapy (ET) for initial treatment and after progression on ET. Abemaciclib has also shown clinical activity in combination with ET in patients with high risk early BC (EBC). Here, we examined the preclinical attributes of abemaciclib and other CDK4 & 6i using biochemical and cell-based assays. In vitro, abemaciclib preferentially inhibited CDK4 kinase activity versus CDK6, resulting in inhibition of cell proliferation in a panel of BC cell lines with higher average potency than palbociclib or ribociclib. Abemaciclib showed activity regardless of *HER2* amplification and phosphatidylinositol 3-kinase (*PI3KCA*) gene mutation status. In human bone marrow progenitor cells, abemaciclib showed lower impact on myeloid maturation than other CDK4 & 6i when tested at unbound concentrations similar to those observed in clinical trials. Continuous abemaciclib treatment provided profound inhibition of cell proliferation, and triggered senescence and apoptosis. These preclinical results support the unique efficacy and safety profile of abemaciclib observed in clinical trials.

Body

Introduction

Breast cancer is the second most common cancer worldwide (1). Pharmacologically targeting cyclin-dependent kinase 4 and 6 (CDK4 & 6) has proven to be a successful therapeutic

33 approach in patients with estrogen receptor-positive (ER+) breast cancer (2). D-type cyclins
34 bind and activate CDK4 & 6. Once active, the holoenzyme phosphorylates the retinoblastoma
35 tumor suppressor protein (Rb), causing the release of transcription factors that promote cell
36 cycle progression to S phase, ultimately leading to cell proliferation (3). CDK4 & 6 are
37 commonly dysregulated in cancer cells, promoting cell proliferation, and suppressing cell
38 senescence (4, 5).

39 To date, the US Food and Drug Administration (FDA) has approved three CDK4 & 6
40 inhibitors (CDK4 & 6i) for treatment of hormone receptor-positive (HR+) metastatic breast
41 cancer (MBC); palbociclib (PD0332991; Ibrance; 6), ribociclib (LEE011; Kisqali; 7) and
42 abemaciclib (LY2835219; Verzenio; 8, 9). Moreover, abemaciclib is the first FDA-approved
43 CDK4 & 6i approved for the adjuvant treatment of HR+, HER2-, node-positive, early breast
44 cancer at high risk of recurrence and a Ki-67 score $\geq 20\%$ (10, 11). Differences have been
45 observed in both efficacy and severity of neutropenia among the available CDK4 & 6i,
46 generating interest in a possible mechanistic explanation (12).

47 Abemaciclib is an ATP-competitive, reversible, selective CDK4 & 6i, which when
48 administered as monotherapy, had a safety profile enabling continuous dosing in a Phase 1
49 clinical study (NCT01394016) (13). The findings were observed in previously treated patients
50 with HR+ MBC, non-small cell lung cancer, and melanoma (14). Moreover, antitumor activity
51 of abemaciclib as a single agent in HR+, HER2- MBC has been demonstrated in a Phase 2
52 trial (NCT02102490) (15). The efficacy and safety of combining abemaciclib plus endocrine
53 therapy (ET) in HR+ MBC has also been demonstrated in key Phase 3 trials, MONARCH 2
54 and MONARCH 3 (16, 17). Abemaciclib is the only CDK4 & 6i to demonstrate significant
55 invasive disease-free survival improvement in the adjuvant treatment of patients with high risk,
56 early breast cancer (EBC) when administered with standard ET (18).

57 Based on previously reported differences between CDK4 & 6i, their efficacy, and their
58 impact on neutropenia, this study examined the preclinical biochemical and cellular profiles of
59 abemaciclib, palbociclib, and ribociclib in a panel of BC cell lines, their impact on neutrophil
60 maturation and the results of intermittent versus continuous treatment. Our results
61 demonstrate that abemaciclib has unique pharmacological properties that are consistent with
62 the safety/efficacy profile observed in clinical trials.

63

64 **Materials & Methods**

65 **Ethics statement**

66 Samples included in this study were provided by the Biobank Hospital Universitario Puerta de
67 Hierro Majadahonda (HUPHM)/Instituto de Investigación Sanitaria Puerta de Hierro-Segovia

68 de Arana (IDIPHISA) (PT17/0015/0020 in the Spanish National Biobanks Network). Samples
69 were processed following standard operating procedures with the appropriate approval of the
70 Ethics and Scientific Committees.

71

72 **Human blood samples**

73 Human whole blood was obtained from six healthy donors who previously provided written
74 informed consent. Mature neutrophils were isolated from human whole blood, using a
75 negative-selection technique (MACSxpress isolation kit, Miltenyi 130-104-434). CD16 cell
76 surface expression (Miltenyi, 130-113-396) was used as quality control; only samples with
77 yield > 95% passed QC. CD34+ human bone marrow primary progenitor cells were obtained
78 from Tebu bio (BM34C-4).

79

80 **Materials**

81 Unless otherwise indicated, all preclinical data described herein were obtained using the
82 methanesulfonate salt of each compound for abemaciclib and palbociclib, and the succinate
83 salt for ribociclib. Full chemical names have been previously published (19).

84 See Supplementary Materials for full list of materials.

85

86 **Biochemical characterization**

87 ***TR-FRET assays***

88 Compounds were mixed with kinase solution at 37.5X final assay concentration and 1%
89 dimethyl sulfoxide (DMSO) and incubated for 30min. Then, the reactions were rapidly diluted
90 in a saturating concentration of ATP and the TR-FRET signal was measured continuously in
91 a multiplate reader Envision (Perkin Elmer).

92 The signal of the baseline control was subtracted from the maximum signal (without
93 compound), as well as from each test compound value. This corrected emission ratio (ER^*)
94 was used to calculate the percentage of activity recovery for each condition:

$$95 \text{ Activity recovery (\%)} = 100X [(compound ER^* - \min control ER^*) / (\max control ER^* - \min \\ 96 \text{ control ER}^*)]$$

97 K_i values were calculated using the following equation: $K_i = IC_{50} / [1 + (S / K_m)]$

98 To measure IC_{50} values using TR-FRET, a LANCE® Ultra kinase assay was used. 5 μ L of test
99 compound was mixed with 5 μ L of kinase and 5 μ L substrate-antibody mixture. Sample
100 containing the peptide, ATP, antibody, and kinase without inhibitor were used as the high
101 reaction control and wells containing the peptide, ATP, and antibody were used as the low
102 reaction control. Test compounds were pre-incubated with the kinase for 30min. The

103 substrate-antibody solution was then added and incubated 1h at room temperature (RT). Test
104 compounds were run in duplicate. Assay was read in a multiplate reader Envision (Perkin
105 Elmer). Results were fitted to a dose-response curve with variable slope and constraints of 0
106 and 100 for bottom and top, respectively, to generate the IC₅₀ values.

$$107 \quad y = Bottom + \frac{Top - Bottom}{1 + 10^{(logIC_{50} - x) \times HillSlope}}$$

108 **Filter binding (FB) assays**

109 Compounds were mixed with substrate mix (C-terminal retinoblastoma fragment [CTRF]
110 peptide and ATP/33-P ATP) at a final concentration range of 2 μM-0.1 nM. The mix was
111 incubated for 90min at RT and the reaction was then stopped by adding 80 μl of 10% ortho-
112 Phosphoric acid. The mix was next transferred to Multiscreen filter plates (Millipore) to retain
113 phosphorylated peptide. The plates were read in a Microbeta Trilux instrument. Reaction mix
114 with excess of EDTA was used as assay “bottom signal”; complete reaction mix without the
115 inhibitor/compound was used as assay “top signal”.

116 For IC₅₀ determination, results were fitted to a four-parameter dose-response curve using the
117 following equation:

$$118 \quad Y = bottom + \frac{(top - bottom)}{1 + (x/IC_{50})^{slope}}$$

119 For the ATP saturation studies K_i and K'_i parameters were estimated using the formula:

$$120 \quad v = V_{max} \frac{[S]}{[K_m (1 + [I]/K_i) + [S] (1 + [I]/K'_i)]}$$

121

122 **Cell lines and culture condition**

123 A panel of 37 BC cell lines (see Table S3 for details) was obtained from the American Type
124 Culture Collection (ATCC, Manassas, Virginia, USA 30-4500 K) or the German Collection of
125 Microorganisms and Cell Cultures GmbH (DSMZ). Cells were cultured according to ATCC or
126 DSMZ recommendations for fewer than ten passages. Cells were seeded in 96 or 384-well
127 plates and incubated overnight prior to treatment.

128 CD34+ cells (Figure 3, S4-6) were thawed and resuspended in IMDM, 10% hiFBS (Fisher),
129 and 1% Pen/Strep (Invitrogen), supplemented with GM-CSF 10 ng/ml, G-CSF 10 ng/ml, SCF
130 100 ng/ml, IL3 10 ng/ml and IL6 10 ng/ml.

131 Mature neutrophils were plated in a 96-well plate (60K cells per well) in 100 μl RPMI 1640
132 (Invitrogen), 10% hiFBS (Fisher) and 1% Pen/Strep (Invitrogen).

133

134 **In vitro drug treatment**

135 ***Breast Cancer Cell panel***

136 Cells were plated at 1,000 or 2,000 cells per well in 384-well plates in a total volume of 25 μ l
137 of either growth media alone; with 2 μ M staurosporine; or with decreasing concentrations of
138 test compounds with a range 2 μ M-0.1 nM. Test compounds were prepared in 100% DMSO
139 using a dilution factor of 1:3 before addition to the cells pre-diluted in growth media. Cells were
140 incubated at 37°C until the untreated cells had doubled twice. Cells were fixed with 70%
141 ethanol, treated with RNase and nuclei stained with Propidium Iodide (PI). Cell nuclei per well
142 were counted using an ACUMEN EXPLORER™ (STP LABTECH LTD) to determine the
143 number of cells remaining after treatment.

144 ***Mature neutrophils from blood***

145 Neutrophils were plated in a 96-well plate (60K cells/well) in the above-mentioned cell medium.
146 A 10 mM stock of each CDK4 & 6i was used to make ten-point 1:3 serial dilutions in 100%
147 DMSO; multiple dilution steps were used to reach the concentration in the assay: 10 μ M, 0.1%
148 DMSO. Non-treated cells (0.1% DMSO) and roscovitine (20 μ M) were used as controls.
149 Neutrophils were incubated for 6 h. Following treatment, cells were washed with FACS flow
150 (BD, 342 003), and supernatant was removed. The cell pellet was stained with Annexin V-
151 FITC antibody for 10 min in the dark. Cells were washed with Annexin buffer, centrifuged at
152 300 G for 5min, supernatant was discarded, and cell pellet was resuspended in 100 μ l of
153 Annexin buffer and analyzed by flow cytometry. PI 1:200 was added automatically by the
154 cytometer. All incubations occurred at 37°C, 5%CO₂.

155 The percentage of alive, early apoptosis, late apoptosis, and dead cells was monitored
156 using the Annexin V/PI assay. Cells were incubated with an anti-human Annexin V-FITC
157 antibody, binding specifically to phosphatidylserine (PS), for 10 min in the dark. PS
158 redistributes to the outer part of the cell membrane in an early stage of apoptosis; in late
159 apoptotic cells, as the cell membrane loses its integrity, both PS and PI can be detected. Thus,
160 the four different phases of apoptosis can be distinguished using flow cytometry technology:
161 Annexin V-/PI- corresponds to alive cells, Annexin V+/PI- corresponds to early apoptotic cells,
162 Annexin V+/PI+ corresponds to late apoptotic cells and Annexin V-/PI+ corresponds to the
163 dead subpopulation of cells. The total number of cells (early, late and dead cells) are
164 represented.

165 ***CD34+ bone marrow progenitor cells***

166 CD34+ progenitor cells were exposed to abemaciclib, palbociclib or ribociclib and the amount
167 of cells/ml were measured after 13 days. On Day 0, 5 000 CD34+ progenitor cells/well were
168 seeded in a deep well plate and were incubated overnight. On Day 1, cell medium was
169 changed for IMDM, 10% hiFBS (Fisher) and 1% Pen/Strep (Invitrogen), supplemented with

170 GMCSF 10 ng/ml, G-CSF 10 ng/ml, SCF 100 ng/ml, IL3 10 ng/ml and IL6 10 ng/ml. Cells were
171 treated with DMSO (vehicle) or with 3-fold dilutions of compounds (abemaciclib, palbociclib,
172 or ribociclib) at a range of concentrations of 20 μ M-1 nM and incubated for 13 days. On Days
173 3, 6 and 10 the cell medium and compounds were renewed (Days 3&6) or supplemented (Day
174 10) to maintain an optimal cell density. To compare the effects of each individual compound
175 at the Cmax, fraction unbound, results at 26 nM (abemaciclib and all active metabolites),
176 38 nM (palbociclib) or 1 548 nM (ribociclib) were interpolated (14, 20-23).

177 ***T47D cells: Continuous dosing***

178 T47D cells were seeded in six-well plates (50 000 cells/well) in 2 ml of cell medium (10%
179 hiFBS [Fisher] and 1% Pen/Strep [Invitrogen]). On Day 1, cells were dosed with abemaciclib
180 or palbociclib at 250 nM, 100 nM or 50 nM final concentrations. Non-treated cells (0.04%
181 DMSO) and staurosporine 1 μ M were used as controls for minimum and maximum inhibition
182 controls respectively. After 2, 6, or 9 days of incubation, cell medium in supernatant was
183 collected and transferred to a deep well plate. Cells were then detached using trypsin and
184 transferred to the deep well plate and spun at 1 300 rpm for 5 min. Cell pellet was washed
185 using PBS1X and plated for apoptosis measurement (Annexin V/PI), using the procedure
186 described above (mature neutrophils). All cells were gated on FSC/SSC to exclude debris and
187 doublets.

188 ***T47D cells: Washout study***

189 100 000 T47D cells/well (short treatment) or 15 000 T47D cells/well (long treatment) were
190 seeded in six-well plates (Thermo Fisher, 140675) in 2 ml of cell medium (10% hiFBS [Fisher]
191 and 1% Pen/Strep [Invitrogen]). The plates were incubated overnight. On Day 1 cells were
192 dosed with 100 nM or 50 nM of abemaciclib or palbociclib as a single treatment or in
193 combination with 5 nM of 4OH-tamoxifen in triplicates. Non-treated cells (DMSO 0.1% as
194 vehicle), as well as staurosporine (100 nM) or Mytomyacin C (200 nM), were used as controls.
195 After 2 or 8 days of continuous treatment the compounds were removed, and cells were
196 incubated with cell medium for four more days. On Days 2 or 8 of continuous treatment, or 4
197 days after compound removal, cells were detached using Accutase for 10 min. All
198 supernatants were collected during the detachment steps to prevent the loss of cells in the
199 suspension. Cells were transferred to a deep well plate and divided into four aliquots for
200 analysis. Cell sensitivity, apoptosis, and senescence were measured by number of cells
201 (remaining after treatment), Annexin V/PI, or cell even green assays respectively. Mitosox was
202 also measured (Sup. Mat.).

203 For fluorescent detection of β -galactosidase, cells were washed with PBS 1X and fixed
204 with 2% PFA (Acros organics, 119690010) for 10 minutes. Cells were then washed with
205 PBS+1%BSA and incubated with the cell even green reagent (Thermo, C10841) following the

206 vendors indications (2h, 31°C, no CO₂). Finally, cells were washed and resuspended in 1%
207 BSA in PBS for FACS analysis (488-nm laser and 525/50 nm filter).

208 For cell proliferation inhibition (cell number), data was normalized versus non-treated cells and
209 staurosporine-treated cells and the percentages were plotted with Graph Pad v8.4.3.

210 Senescence (cell even green) was represented as the percentage of green positive cells and
211 compared to non-treated cells.

212

213 **Western blot**

214 Cells were washed with PBS and lysed with ice-cold lysis buffer containing 2 mM PMSF,
215 10 mM EDTA, and 2xHalt protease and phosphatase inhibitor cocktail (Thermo). After a
216 10 min incubation on ice, the lysate was centrifuged at 14 000 rpm at 4°C for 5 min. The
217 supernatant was stored in –80°C for Western blotting. 45µg of each sample quantified by BCA
218 assay was loaded onto NuPAGE 4% to 12% Bis-Tris Gel and immobilized onto nitrocellulose
219 membrane using Tris-Glycine transfer buffer at 100 V for 1 h. The immunoblotting was
220 performed in a blocking buffer of 2.5% non-fat milk/TBS-T and detected by anti-CDK4 antibody
221 and anti-CDK6 antibody using ECL-HRP on Fujifilm LAS4000.

222

223 **Analysis and statistical considerations**

224 Raw data were analyzed with FlowJo 10.6 software. Graph Pad v8.4.3 software was used for
225 data analysis and representation of final readouts. JMP (Statistical Discovery from SAS) was
226 used for the statistical treatment (ANOVA, pairwise analysis) of the data.

227 The IC₅₀ was determined by curve fitting to a four-parameter logistic equation for each output
228 using GENEDATA SCREENER® tool: or GraphPad Prims®.

$$229 \quad Y = \text{bottom} + \frac{[(\text{top}-\text{bottom})/1+(x/ \text{IC}_{50}) \text{ slope}]}{}$$

230 where Y = % inhibition (%Inh = [(median Max- x/ median Max – median Min)]/100], X =
231 concentration yielding y% inhibition.

232 Ten-points curves were obtained and a RelIC₅₀ was calculated.

233 **Flow cytometry analysis.** Cells were analyzed using a flow cytometer (Macsquant Analyzer
234 10, Miltenyi). Events were gated for debris exclusion and singlets selection. A minimum of
235 3 500 cells were analyzed per sample. PI (1:200) was added automatically by the cytometer.
236 Cells negative for Annexin V and PI (% alive cells) were used for analysis. Cells/ml (gated on
237 singlets) were evaluated using the Macsquantify 2.13 software (more details on analyses in
238 Sup. Mat.).

239

240 **Results**

241 **1. *Abemaciclib is a more potent inhibitor of CDK4 than CDK6***

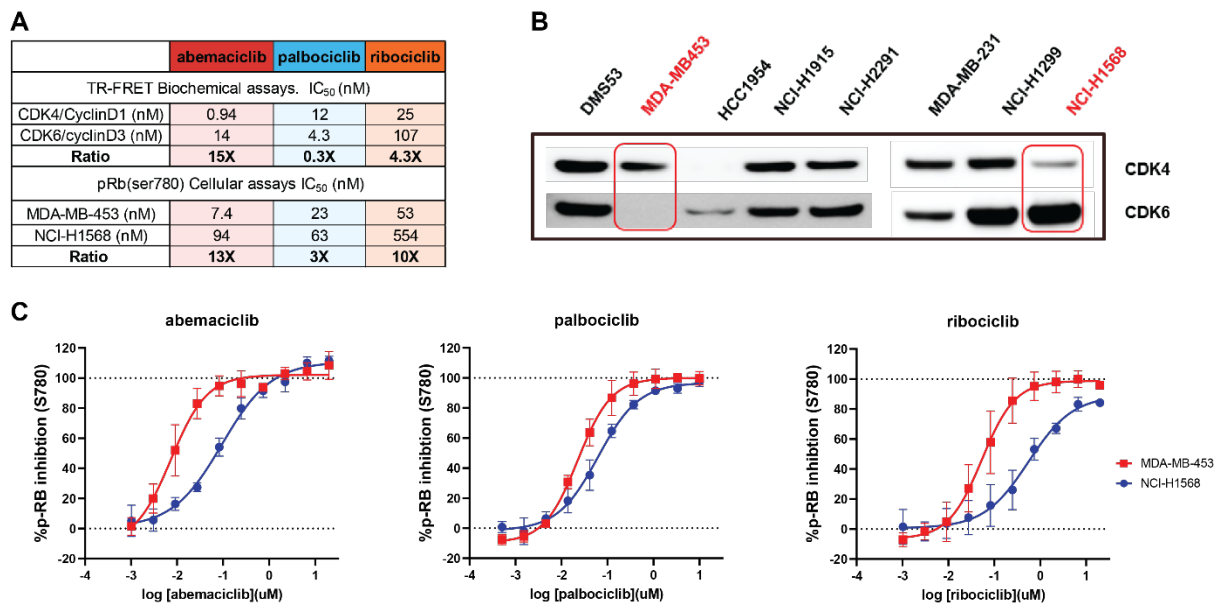
242 The potency of abemaciclib, palbociclib and ribociclib to inhibit CDK4/cyclinD1 and
243 CDK6/cyclinD3 activity was evaluated by measuring retinoblastoma phosphorylation by TR-
244 FRET or FB assays. Abemaciclib is a highly potent inhibitor of CDK4/cyclin D1 showing in TR-
245 FRET assays an IC₅₀ value of 0.94 nM; abemaciclib potency against CDK6/cyclinD3 was
246 14 nM, demonstrating a selectivity ratio CDK4/CDK6 of 15-fold. In contrast, palbociclib yielded
247 a selectivity ratio CDK4/CDK6 of 0.3-fold and ribociclib 4.3-fold (Figure 1A). These results
248 were consistent regardless of the method used (FB assays IC₅₀ or Ki determination by FB or
249 TR-FRET; Table S1).

250 These results were confirmed in an isoform-specific cellular context using cell models
251 that are dependent on CDK4 or CDK6, according to the relative expression of each kinase
252 (Figure 1B). Intracellular phosphorylation of Rb in its residue 780 (Ser780) was measured
253 using fluorescently labeled phospho-specific antibodies and high content imaging.
254 Abemaciclib showed a dose-response inhibition of the Rb phosphorylation in the CDK4-
255 dependent cell line MDA-MB-453 (Figure 1B) with a potency of 7.4 nM, and in the CDK6
256 dependent cell line NCI-H1568 with a potency of 94 nM (Figure1A-C), which translates to a
257 selectivity ratio CDK4/CDK6 of 13-fold. In contrast, in same cellular environment, palbociclib
258 and ribociclib showed lower potency 23 nM and 53 nM with a selectivity ratio of 3-fold and 10-
259 fold, respectively. (Figure1C). CDK4 dependency in this cell line was confirmed by knocking
260 out CDK4 or CDK6 by shRNA (Figure S2A). The higher potency shown by abemaciclib in
261 inhibiting Rb phosphorylation was reproducible across several breast cancer cell lines (Table
262 S2).

263 Additionally, to understand whether the profound inhibition of CDK4 may results in a
264 more durable response, the effects of abemaciclib and palbociclib on Rb phosphorylation were
265 assessed in an in vitro washout experiment (Figure S1A). In the breast cancer cell line MDA-
266 MB-453, intracellular CDK4 activity was functionally inhibited during the treatment phase, as
267 observed by the complete depletion of pRb (Ser780) regardless of treatment (Figure S1B).
268 Under these conditions, both compounds showed relative IC₅₀ values for pRb (Ser780)
269 reduction in the low nM range: 6.4 nM for abemaciclib and 14.1 nM for palbociclib (Figure
270 S1C). After compound removal, Rb phosphorylation was recovered in cells previously
271 exposed to palbociclib, but not in those treated with abemaciclib, which maintained a relative
272 IC₅₀ below 100 nM even 12 h after compound removal. In cells pre-treated with palbociclib,
273 relative IC₅₀ increased to 446.7 nM 12 h after compound removal (Figure S1B-C). Taken

274 together, those results demonstrate the sustained target inhibition and longer-term effect of
 275 abemaciclib in ER+ BC cell lines.

276



277

278 **Figure 1. Abemaciclib is a more potent inhibitor of CDK4 than CDK6 in both biochemical**
 279 **and in vitro cell-based assays.** In a head-to-head comparison, abemaciclib showed higher
 280 potency to inhibit CDK4 than CDK6 with a broader margin of selectivity than other CDK4 and
 281 CDK6 inhibitors. This was confirmed in biochemical assays and in cellular systems.
 282 Biochemical potency (KiATP) and selectivity ratio CDK6/CDK4 (additional IC₅₀ values, FB
 283 assay and TR-FRET in Supplemental Material) as cell assays for abemaciclib and palbociclib
 284 are included in **table A**). Figure **1B**) represents the Western Blot showing the expression of
 285 CDK4 and CDK6 in different cell models. MDA-MB-453 and NCI-H1568 cells (highlighted)
 286 showed preferential expression of CDK4 or CDK6 respectively. **(C)** Dose-response curves of
 287 abemaciclib, palbociclib, and ribociclib showing inhibition of Rb (retinoblastoma) ser780
 288 phosphorylation, quantitated intracellularly by high content imaging in CDK4 and CDK6
 289 dependent cell models (MDA-MB-453 and NCI-H1568) Data reported as an average of four
 290 independent determinations (n = 4) ± standard deviation (SD; error bars).

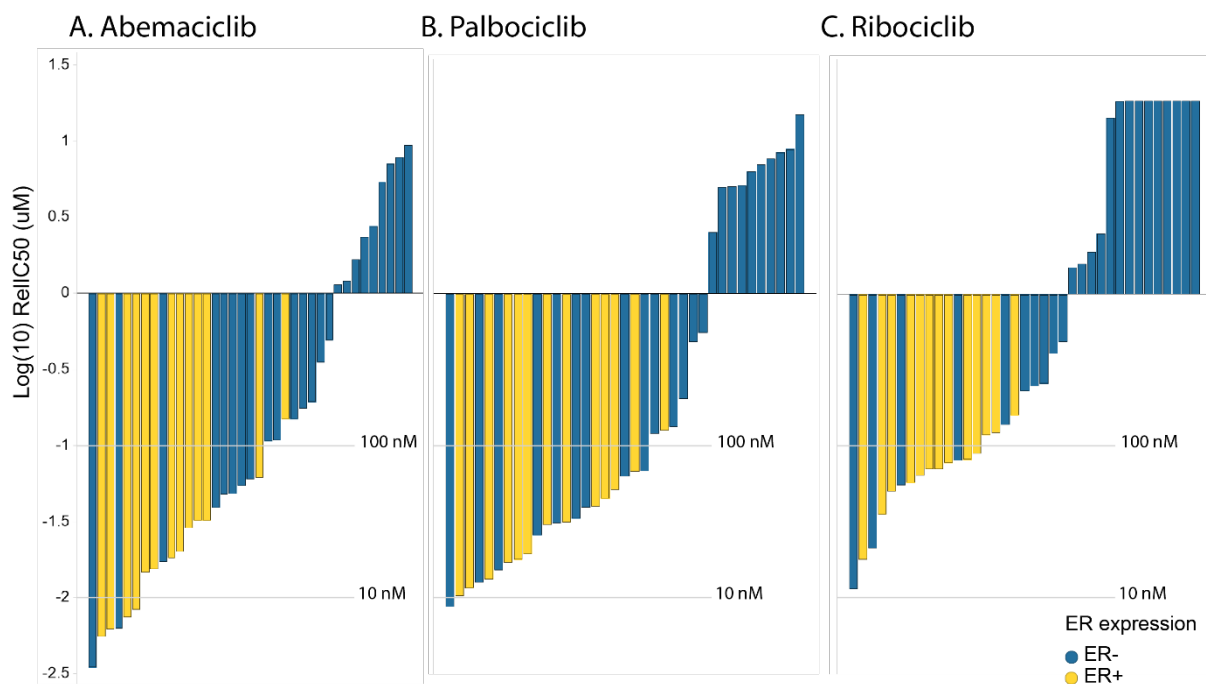
291 TR-FRET: Time-Resolved Foerster Resonance Energy Transfer; FB: Filter Binding.

292

293 2. **Abemaciclib is a potent inhibitor of proliferation in breast cancer cell lines**

294 The impact of the three CDK4 & 6i on both mature neutrophils and myeloid maturation was
 295 investigated in vitro to gain insights on the effects in hematopoietic cells at a concentration
 296 similar to the plasma levels of these inhibitors in clinical trials. For abemaciclib, we combined
 297 the parent molecule with its two active circulating metabolites with equivalent pharmacology
 298 (14, 20-23). At the concentration (corrected for protein binding) equivalent to the average

299 clinical Cmax reported for each CDK4 & 6i (unbound Cmax), there was no impact on circulating
300 neutrophils in blood (Figures 3A-B). However, the impact on the maturation of progenitor cells
301 from bone marrow was lower with abemaciclib treatment compared with palbociclib or
302 ribociclib (Figures 3C-D). Furthermore, in human bone marrow progenitor cells, abemaciclib
303 triggered apoptosis with lesser extent than palbociclib (Figure S4) and had also a lesser impact
304 on neutrophil maturation markers (Figure S5). Importantly, neither known abemaciclib
305 metabolites nor combination of abemaciclib with fulvestrant had any impact on neutrophils
306 maturation in vitro (Figures S5 and S6).
307



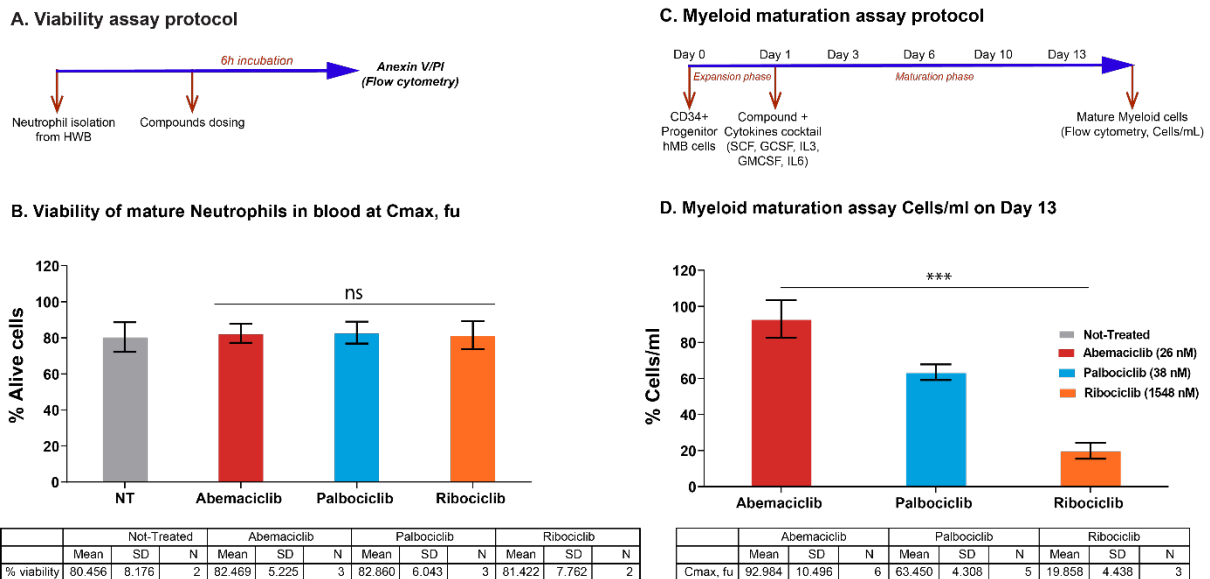
308
309 **Figure 2. Abemaciclib shows greater potency than palbociclib & ribociclib in breast**
310 **cancer cells.** In vitro drug response waterfall plots for (A) abemaciclib, (B) palbociclib, (C) or
311 ribociclib in a panel composed of 40 cell lines, either ER- (blue) or ER+ (yellow). Bar graph of
312 log IC₅₀ values (uM) and cell type. Cell lines are color coded by subtype: yellow is luminal ER+;
313 blue is ER-. Waterfall plots were generated using the geometric mean for each cell line and
314 treatment.

315

316 3. ***Abemaciclib showed a lesser impact on myeloid maturation than other CDK4*** 317 ***& 6 inhibitors***

318 The impact of the three CDK4 & 6i on both mature neutrophils and myeloid maturation was
319 investigated in vitro. At the Cmax fraction unbound for each CDK4 & 6i (14, 20-23), there was
320 no impact on circulating neutrophils in blood (Figures 3A-B). However, the impact on the
321 maturation of progenitor cells from bone marrow was lower with abemaciclib treatment

322 compared with palbociclib or ribociclib (Figures 3C-D). Furthermore, in human bone marrow
 323 progenitor cells, abemaciclib triggered apoptosis with lesser extent than palbociclib (Figure
 324 S4) and had also a lesser impact on neutrophil maturation markers (Figure S5). Importantly,
 325 neither known abemaciclib metabolites nor combination of abemaciclib with fulvestrant had
 326 any impact on neutrophils maturation in vitro (Figures S5 and S6).
 327



328 **Figure 3. Impact on neutrophils maturation is lower upon abemaciclib treatment**
 329 **comparing with others CDK4 & 6 inhibitors in preclinical models. (A-B)** Viability of
 330 isolated mature neutrophils from human whole blood at Cmax, fu. **(C-D)** Myeloid maturation
 331 assay, measuring cells per mL on Day 13. Data are plotted as the mean +/-SD of more than
 332 two independent replicates.
 333

334 HWB: Human Whole Blood, hBM: human Bone Marrow, PI: Propidium Iodide, Cmax,fu: maximum unbound
 335 concentration in plasma.

336 *** p-value < 0.0001; ns. or no *: non-significant. One way ANOVA among three groups. In a pairwise comparison
 337 there is a size effect of 18.54 for abemaciclib versus palbociclib and 61.99 for abemaciclib versus ribociclib with p-
 338 values of 0.0035 and < 0.0001 respectively.

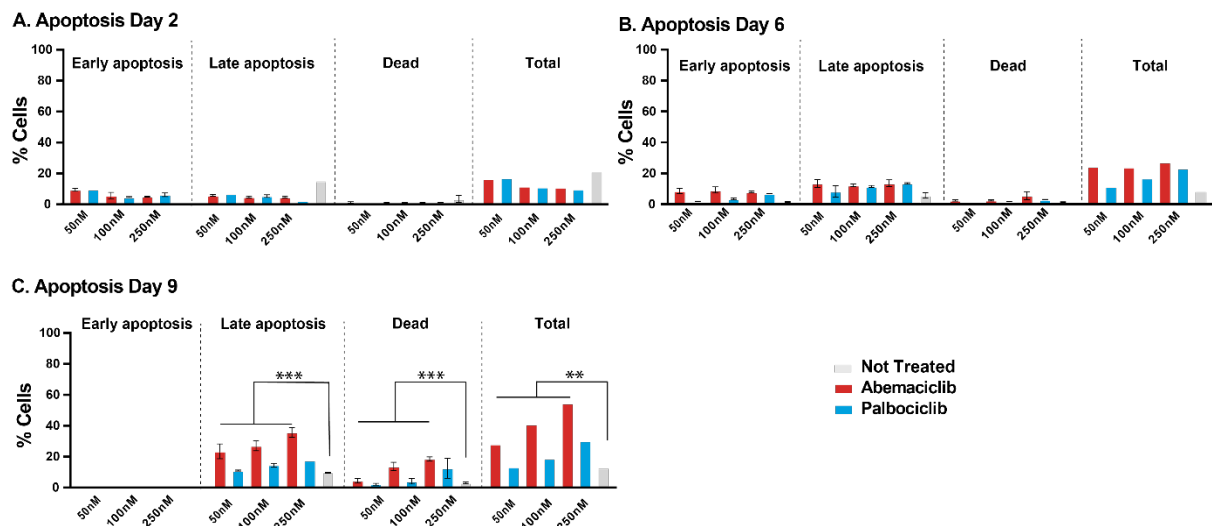
339

340 **4. Prolonged treatment with abemaciclib leads to apoptosis**

341 To understand the impact of longer treatment of abemaciclib and palbociclib on their efficacy
 342 in breast cancer cell lines, a time course (2, 6 and 9 days) at 50, 100 and 250 nM was
 343 performed to evaluate the biological effect by flow cytometry, early (PI-/Annexin V+) and late
 344 apoptosis (PI+/Annexin V+), and cell death (PI+/Annexin V-) events (Figure 4). Early
 345 apoptotic effects are observed at Days 2 and 6, and late apoptotic effects are significant
 346 upon 9 days of treatment (Figure 4). Although the increase of apoptosis is observed upon

347 both CDK4 and CDK6 inhibitors after 8 days of continuous dosing, the percentage in total
348 apoptotic and dead cells is higher upon abemaciclib treatment compared with palbociclib at
349 the two concentrations tested (28.1% versus 13.2% at 50 nM; 40.7% versus 18.7% at
350 100 nM, for abemaciclib and palbociclib, respectively). Taken all those data together we
351 conclude that prolonged treatment with abemaciclib promoted dose-dependent apoptosis in
352 T47D (Figure 4) and MCF7 breast cancer cells (data not shown).

353



354

355 **Figure 4. Prolonged treatment of breast cancer cells with a CDK4 & 6 inhibitor is**
356 **necessary to sustain cell growth inhibition and promote apoptosis.** T47D cells were
357 treated with DMSO, 50, 100 or 250 nM of the CDK4 & 6i abemaciclib or palbociclib for 2, 6,
358 and 9 days. **(A-C)** percentage of apoptotic cells are monitored by Annexin V and PI. The data
359 are plotted as the mean (+/- SD) of three experiments for CDK4 & 6i treatment, and the mean
360 of three experiments (+/- SD) for untreated samples.

361 ANOVA analysis of Day 6 data show that % cell in apoptosis (late, total, or dead) is significantly
362 different between groups treated with abemaciclib or not treated (FC 2.9, 3.1 and 3.3
363 respectively); % cell in late apoptosis is significantly different between groups treated with
364 palbociclib or not treated (FC 1.45), although there is not significant change in the case of total
365 apoptosis or dead cells in groups treated with palbociclib or not treated (FC 1.51 and 1.48
366 respectively).

367 ANOVA: Analysis of Variance, SD: Standard deviation, FC: Fold Change. *** p-value ≤ 0.0001 , ** p-value ≤ 0.001 ;
368 if no p-value presented, the differences between groups were not statistically different.

369

370 5. Permanent exposure leads to durable effects after compound removal

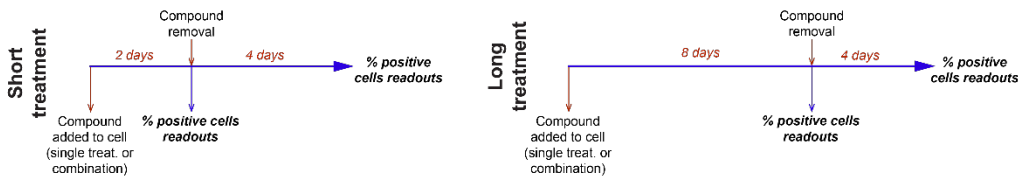
371 To compare the persistence of effects after compound removal, T47D cells (ER+, PR+,
372 HER2-) were treated with a CDK4 & 6i (abemaciclib or palbociclib) as monotherapy or in

373 combination with tamoxifen for 2 to 8 days (Figure 5A). Compounds were then removed, and
374 cells were incubated for 4 more days. Cell proliferation, senescence and apoptosis were
375 monitored (Figure 5 and Figures S7&S8). Overall, the effect was more durable when cells had
376 previously been treated for longer (8 days). Nevertheless, it is worth highlighting that after 2-
377 day treatment with abemaciclib plus tamoxifen, a higher cell proliferation inhibition was
378 observed (Figure 5B), which is consistent with previous data obtained in monotherapy (Figure
379 S8A).

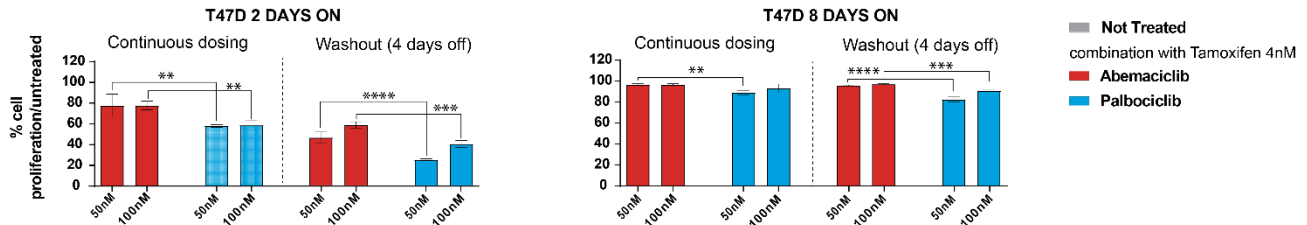
380 When comparing the different treatments, no significant difference in cell number
381 inhibition after compound removal (8-day treatment + 4-day WO) was observed with tamoxifen
382 plus either abemaciclib or palbociclib (Figure 5B). However, the number of senescent cells
383 remained significantly higher with the combination of abemaciclib + tamoxifen compared to
384 combinations with palbociclib (Figure 5C). A significant number of apoptotic cells remained
385 after compound removal (8-day treatment + 4-day WO; Figure 5D). These results were
386 consistent regardless of the methodology used (cell even green or Mitosox) and similar results
387 were observed with monotherapy treatments (Figure S8) or in combination with fulvestrant
388 (data not shown).

389

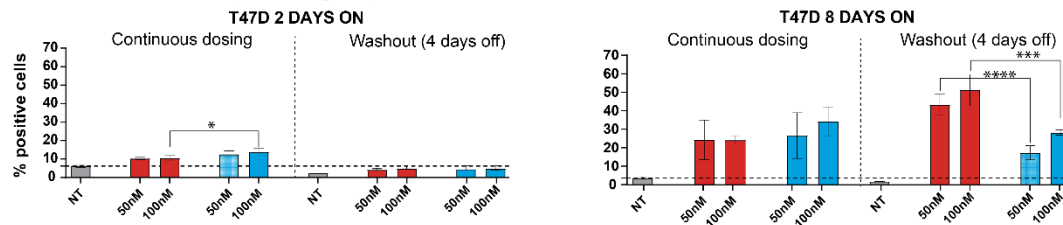
A. WASHOUT STUDY



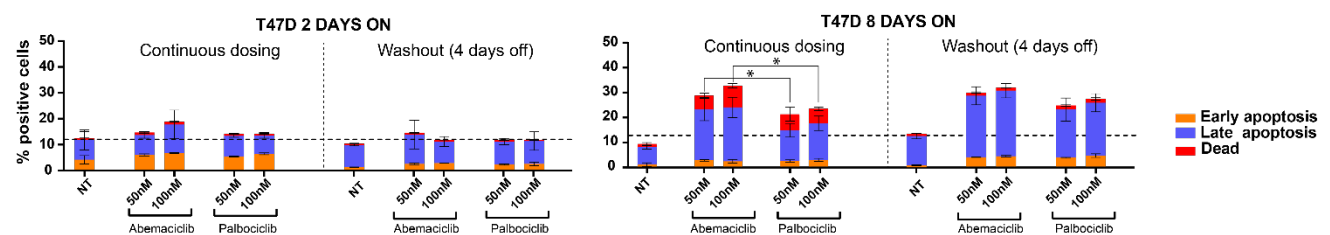
B. CELL PROLIFERATION INHIBITION (cell number)



C. CELL SENEESCENCE (cell even green)



D. APOPTOSIS (Anexin V/PI)



390 **Figure 5. Washout studies demonstrated durable effects after abemaciclib removal.**

391 Cells treated with either abemaciclib or palbociclib + 5 nM tamoxifen. (A) Cell proliferation
 392 inhibition. (B) Percentages of senescent cells were monitored by cell even green kit. (C)
 393 Percentage of apoptotic cells, monitored by Annexin V and PI. The data are plotted as the
 394 mean (+/- SD) of three experiments.

395 NT: non-treated. * p-value ≤ 0.05 ; ** p-value ≤ 0.01 ; *** p-value ≤ 0.001 ; **** p-value ≤ 0.0001 ; ns. or no *: non-
 396 significant.

397

398 Discussion

399 CDK4 & 6i have demonstrated robust clinical activity, receiving FDA approval for the treatment
 400 of advanced BC (11, 24, 25), and are being further investigated in additional clinical trials.
 401 Here, we examined the preclinical biochemical and cellular profiles of abemaciclib, palbociclib,
 402 and ribociclib in a panel of BC cell lines, neutrophils, and bone marrow progenitor cells. We
 403 studied the activity profile of each agent in broad panels of BC cells in single treatment, as
 404 well as in different dose regimen schedules.

405 In cell-free assays, abemaciclib showed selectivity for CDK4 over CDK6; in cell-based
406 assays, it preferentially inhibited the proliferation of cells dependent on the presence of CDK4,
407 not CDK6, and it showed to be a more potent CDK4 inhibitor and selective against CDK6 than
408 palbociclib and ribociclib (26)(Figure 1, Table S1). The biochemical profile translated to cell-
409 based assays, with CDK4-dependent breast cancer cell lines showing a profound inhibition of
410 pRb under abemaciclib treatment. Robust cell cycle arrest, through inhibition of pRb,
411 correlated with potent inhibition of cell proliferation in a large panel of BC cell lines. For
412 instance, abemaciclib demonstrated greater potency than palbociclib and ribociclib in BC cell
413 lines, regardless of ER positivity. Additionally, abemaciclib potently inhibited cell proliferation
414 in BC cell lines, regardless of *HER2* amplification or *PI3KCA* and *BRCA1/2* gene mutation
415 status.

416 Clinically, lower incidence and severity of neutropenia was reported in patients receiving
417 abemaciclib treatment, compared to patients receiving either palbociclib or ribociclib (14, 27).
418 The relationship of CDK6 and cyclinD3 in the maturation of the myeloid cells has been broadly
419 discussed and demonstrated in preclinical studies with transgenic mice models lacking either
420 CDK4 or CDK6 in adult hematopoiesis (28-31). In vitro, we investigated the impact of the three
421 CDK4 & 6i on both mature neutrophils and the myeloid maturation. None of the CDK4 & 6i
422 impacted mature circulating neutrophils in the bloodstream; however, abemaciclib treatment
423 resulted in a lower impact on the maturation process compared to palbociclib and ribociclib,
424 which may contribute to lower incidence of neutropenia. The higher and more selective activity
425 of abemaciclib against CDK4 than CDK6 (Figure 1, Table S1), as well as the ratio of unbound
426 C_{max} to CDK6 potency, may explain the different rates of neutropenia observed among
427 treatments (14). The differentiated pharmacological profile of abemaciclib may contribute to
428 its tolerability profile that allows for continuous dosing whereas palbociclib and ribociclib need
429 to be administered intermittently.

430 In vitro, treatment with abemaciclib and palbociclib inhibited cell proliferation by inhibiting Rb
431 phosphorylation. After compound removal, Rb phosphorylation inhibition was maintained only
432 in cells treated with abemaciclib, demonstrating the sustained target inhibition and longer-term
433 effect of abemaciclib in ER+ BC cell lines. Consistent with this observation, T47D cells treated
434 with abemaciclib were inhibited for longer, after compound removal, than cells treated with
435 palbociclib. The anti-proliferative activity of abemaciclib thus had a more durable effect in
436 promoting apoptosis, emphasizing the importance of efficient target inhibition in leading to a
437 durable cellular response. Continuous treatment with abemaciclib promoted a greater
438 response than intermittent treatment, as monitored by remaining cell number, senescence,
439 and cell apoptosis. This suggests that continuous treatment is required to observe complete
440 senescence and irreversible effects through apoptosis. We conclude that in preclinical models,

441 continuous treatment with abemaciclib is required for profound and sustained effects, resulting
442 in superior activity.

443

444 **Conclusion**

445 In preclinical experiments, abemaciclib is a potent, selective cell growth inhibitor, inhibiting
446 preferentially the CDK4/Cyclin D1 complex and leading to cell senescence and cell death in
447 breast cancer cell lines with broad molecular profiles. Abemaciclib has a lesser impact on
448 neutrophils maturation in vitro than other CDK4 & 6, which is consistent with lower incidences
449 of neutropenia observed in clinical settings and may allow for a prolonged treatment. After
450 prolonged dosing with abemaciclib, cells show sustained inhibition of cell proliferation that
451 leads to irreversible effects through apoptosis. These preclinical results support the
452 differentiated safety and efficacy profile of abemaciclib observed in clinical trials.

453 **Table of Abbreviations**

454	ATCC	American Type Culture Collection
455	BC	Breast cancer
456	BCA	Bicinchoninic acid
457	CTRF	C-terminal retinoblastoma fragment
458	DMSO	Dimethyl sulfoxide
459	DSMZ	German Collection of Microorganisms and Cell Cultures GmbH
460	EDTA	Ethylenediaminetetraacetic acid
461	ER	Estrogen receptor
462	ET	Endocrine therapy
463	FB	Filter Binding
464	FDA	Food and Drug Administration
465	hBM	Human bone marrow
466	HR	Hormone receptor
467	HWB	Human whole blood
468	IMDM	Iscove's Modified Dulbecco's Medium
469	LRL	Lilly Research Laboratories
470	MBC	Metastatic breast cancer
471	NT	Not treated
472	PBS	Phosphate Buffered Saline
473	PI	Propidium Iodide
474	RT	room temperature
475	SD	Standard deviation
476	TNBC	Triple negative breast cancer
477	TR-FRET	Time-Resolved Foerster Resonance Energy Transfer
478	WO	Washout

479

480 **Acknowledgements**

481 The authors wish to thank the donors, and the Biobank Hospital Universitario Puerta de Hierro
482 Majadahonda (HUPHM)/Instituto de Investigación Sanitaria Puerta de Hierro-Segovia de
483 Arana (IDIPHISA) (PT17/0015/0020 in the Spanish National Biobanks Network) for the human
484 specimens used in this study. The authors thank Eglantine Julle-Daniere for her medical
485 writing and editorial assistance for this manuscript, Dongling Fei for statistical analysis and
486 data representation assistance, and Maria Jesús Ortiz for quality review assistance.

487 **Funding**

488 This work was supported by Eli Lilly and Company.

489 **Disclosures**

490 This work was supported by Eli Lilly and Company. All authors are employees of Eli Lilly and
491 Company and shareholders of Eli Lilly and Company.

492 References

- 493 1. Ferlay J, Soerjomataram I, Dikshit R, Eser S, Mathers C, Rebelo M, et al. Cancer
494 incidence and mortality worldwide: sources, methods and major patterns in GLOBOCAN
495 2012. *International journal of cancer*. 2015;136(5):E359-E86.
- 496 2. Finn RS, Aleshin A, Slamon DJ. Targeting the cyclin-dependent kinases (CDK) 4/6 in
497 estrogen receptor-positive breast cancers. *Breast Cancer Research*. 2016;18(1):1-11.
- 498 3. Harbour JW, Luo RX, Dei Santi A, Postigo AA, Dean DC. Cdk phosphorylation
499 triggers sequential intramolecular interactions that progressively block Rb functions as cells
500 move through G1. *Cell*. 1999;98(6):859-69.
- 501 4. Malumbres M, Barbacid M. Cell cycle, CDKs and cancer: a changing paradigm.
502 *Nature reviews cancer*. 2009;9(3):153-66.
- 503 5. O'Leary B, Finn RS, Turner NC. Treating cancer with selective CDK4/6 inhibitors. *Nat*
504 *Rev Clin Oncol*. 2016;13(7):417-30.
- 505 6. Cristofanilli M, Turner NC, Bondarenko I, Ro J, Im S-A, Masuda N, et al. Fulvestrant
506 plus palbociclib versus fulvestrant plus placebo for treatment of hormone-receptor-positive,
507 HER2-negative metastatic breast cancer that progressed on previous endocrine therapy
508 (PALOMA-3): final analysis of the multicentre, double-blind, phase 3 randomised controlled
509 trial. *The Lancet Oncology*. 2016;17(4):425-39.
- 510 7. Hortobagyi GN, Stemmer SM, Burris HA, Yap YS, Sonke GS, Paluch-Shimon S, et
511 al. Ribociclib as First-Line Therapy for HR-Positive, Advanced Breast Cancer. *New England*
512 *Journal of Medicine*. 2016;375(18):1738-48.
- 513 8. Dickler MN, Tolaney SM, Rugo HS, Cortes J, Dieras V, Patt DA, et al. MONARCH1:
514 Results from a phase II study of abemaciclib, a CDK4 and CDK6 inhibitor, as monotherapy,
515 in patients with HR+/HER2-breast cancer, after chemotherapy for advanced disease.
516 *American Society of Clinical Oncology*; 2016.
- 517 9. Sledge GW, Jr., Toi M, Neven P, Sohn J, Inoue K, Pivot X, et al. MONARCH 2:
518 Abemaciclib in Combination With Fulvestrant in Women With HR+/HER2- Advanced Breast
519 Cancer Who Had Progressed While Receiving Endocrine Therapy. *J Clin Oncol*.
520 2017;35(25):2875-84.
- 521 10. Harbeck N, Rastogi P, Martin M, Tolaney S, Shao Z, Fasching P, et al. Adjuvant
522 abemaciclib combined with endocrine therapy for high-risk early breast cancer: updated
523 efficacy and Ki-67 analysis from the monarchE study. *Annals of Oncology*. 2021.
- 524 11. VERZENIO™ (abemaciclib) [US Package Insert], (2021).
- 525 12. Tamura K. Differences of cyclin-dependent kinase 4/6 inhibitor, palbociclib and
526 abemaciclib, in breast cancer. *Japanese journal of clinical oncology*. 2019;49(11):993-8.
- 527 13. Tate SC, Sykes AK, Kulanthaivel P, Chan EM, Turner PK, Cronier DM. A population
528 pharmacokinetic and pharmacodynamic analysis of abemaciclib in a phase I clinical trial in
529 cancer patients. *Clinical pharmacokinetics*. 2018;57(3):335-44.
- 530 14. Patnaik A, Rosen LS, Tolaney SM, Tolcher AW, Goldman JW, Gandhi L, et al.
531 Efficacy and safety of abemaciclib, an inhibitor of CDK4 and CDK6, for patients with breast
532 cancer, non-small cell lung cancer, and other solid tumors. *Cancer discovery*.
533 2016;6(7):740-53.
- 534 15. Dickler MN, Tolaney SM, Rugo HS, Cortes J, Dieras V, Patt D, et al. MONARCH 1, A
535 Phase II Study of Abemaciclib, a CDK4 and CDK6 Inhibitor, as a Single Agent, in Patients
536 with Refractory HR(+)/HER2(-) Metastatic Breast Cancer. *Clin Cancer Res*.
537 2017;23(17):5218-24.

- 538 16. Johnston S, Martin M, Di Leo A, Im SA, Awada A, Forrester T, et al. MONARCH 3
539 final PFS: a randomized study of abemaciclib as initial therapy for advanced breast cancer.
540 NPJ Breast Cancer. 2019;5:5.
- 541 17. Sledge GW, Jr., Toi M, Neven P, Sohn J, Inoue K, Pivot X, et al. The Effect of
542 Abemaciclib Plus Fulvestrant on Overall Survival in Hormone Receptor-Positive, ERBB2-
543 Negative Breast Cancer That Progressed on Endocrine Therapy-MONARCH 2: A
544 Randomized Clinical Trial. JAMA Oncol. 2020;6(1):116-24.
- 545 18. Johnston SRD, Harbeck N, Hegg R, Toi M, Martin M, Shao ZM, et al. Abemaciclib
546 Combined With Endocrine Therapy for the Adjuvant Treatment of HR+, HER2-, Node-
547 Positive, High-Risk, Early Breast Cancer (monarchE). J Clin Oncol. 2020;JCO2002514.
- 548 19. Gelbert LM, Cai S, Lin X, Sanchez-Martinez C, Del Prado M, Lallena MJ, et al.
549 Preclinical characterization of the CDK4/6 inhibitor LY2835219: in-vivo cell cycle-
550 dependent/independent anti-tumor activities alone/in combination with gemcitabine. Invest
551 New Drugs. 2014;32(5):825-37.
- 552 20. Raub TJ, Wishart GN, Kulanthaivel P, Staton BA, Ajamie RT, Sawada GA, et al.
553 Brain exposure of two selective dual CDK4 and CDK6 inhibitors and the antitumor activity of
554 CDK4 and CDK6 inhibition in combination with temozolomide in an intracranial glioblastoma
555 xenograft. Drug Metabolism and Disposition. 2015;43(9):1360-71.
- 556 21. Flaherty KT, LoRusso PM, DeMichele A, Abramson VG, Courtney R, Randolph SS,
557 et al. Phase I, dose-escalation trial of the oral cyclin-dependent kinase 4/6 inhibitor PD
558 0332991, administered using a 21-day schedule in patients with advanced cancer. Clinical
559 Cancer Research. 2012;18(2):568-76.
- 560 22. Groenland SL, Martínez-Chávez A, van Dongen MG, Beijnen JH, Schinkel AH,
561 Huitema AD, et al. Clinical pharmacokinetics and pharmacodynamics of the Cyclin-
562 dependent kinase 4 and 6 inhibitors Palbociclib, Ribociclib, and Abemaciclib. Clinical
563 Pharmacokinetics. 2020:1-20.
- 564 23. Infante JR, Cassier PA, Gerecitano JF, Witteveen PO, Chugh R, Ribrag V, et al. A
565 phase I study of the cyclin-dependent kinase 4/6 inhibitor ribociclib (LEE011) in patients with
566 advanced solid tumors and lymphomas. Clinical Cancer Research. 2016;22(23):5696-705.
- 567 24. IBRANCE® [US Package Insert], (2016).
- 568 25. KISQALI® (ribociclib) [US Package Insert], (2017).
- 569 26. Hafner M, Mills CE, Subramanian K, Chen C, Chung M, Boswell SA, et al. Multiomics
570 profiling establishes the polypharmacology of FDA-approved CDK4/6 inhibitors and the
571 potential for differential clinical activity. Cell chemical biology. 2019;26(8):1067-80. e8.
- 572 27. Tripathy D, Bardia A, Sellers WR. Ribociclib (LEE011): mechanism of action and
573 clinical impact of this selective cyclin-dependent kinase 4/6 inhibitor in various solid tumors.
574 Clinical Cancer Research. 2017;23(13):3251-62.
- 575 28. Laurenti E, Frelin C, Xie S, Ferrari R, Dunant CF, Zandi S, et al. CDK6 levels
576 regulate quiescence exit in human hematopoietic stem cells. Cell stem cell. 2015;16(3):302-
577 13.
- 578 29. Sicinska E, Lee Y-M, Gits J, Shigematsu H, Yu Q, Rebel VI, et al. Essential role for
579 cyclin D3 in granulocyte colony-stimulating factor-driven expansion of neutrophil
580 granulocytes. Molecular and cellular biology. 2006;26(21):8052-60.
- 581 30. Cooper AB, Sawai CM, Sicinska E, Powers SE, Sicinski P, Clark MR, et al. A unique
582 function for cyclin D3 in early B cell development. Nature immunology. 2006;7(5):489-97.

583 31. Maurer B, Brandstoetter T, Kollmann S, Sexl V, Prchal-Murphy M. Inducible deletion
584 of CDK4 and CDK6-deciphering CDK4/6 inhibitor effects in the hematopoietic system.
585 Haematologica. 2020.
586